Biochemical and Biophysical Research Communications 437 (2013) 87–93

Contents lists available at SciVerse ScienceDirect

Biochemical and Biophysical Research Communications

journal homepage: www.elsevier.com/locate/ybbrc

Piperlongumine selectively kills glioblastoma multiforme cells via reactive oxygen species accumulation dependent JNK and p38 activation

Ju Mei Liu [a,1], Feng Pan [a,b,1], Li Li [a], Qian Rong Liu [a], Yong Chen [a], Xin Xin Xiong [a], Kejun Cheng [c,d], Shang Bin Yu [a], Zhi Shi [e], Albert Cheung-Hoi Yu [f], Xiao Qian Chen [a,*]

[a] Department of Pathophysiology, School of Basic Medicine, Key Laboratory of Neurological Diseases, Ministry of Education, Hubei Provincial Key Laboratory of Neurological Diseases, Huazhong University of Science and Technology, Wuhan 430030, China
[b] Department of Urology, Union Hospital, Huazhong University of Science and Technology, Wuhan 430030, China
[c] Chemical Biology Center, Lishui Institute of Agricultural Sciences, Lishui, Zhejiang 323300, China
[d] Vatalis Tech, LLC, Houston, TX 77054, USA
[e] Department of Cell Biology & Institute of Biomedicine, College of Life Science, Jinan University, Guangzhou 510632, China
[f] Neuroscience Research Institute & Department of Neurobiology, School of Basic Medical Sciences, Key Laboratory for Neuroscience, Ministry of Education/National Health and Family Planning Commission, Peking University, Beijing 100191, China

ARTICLE INFO

Article history:
Received 10 June 2013
Available online 22 June 2013

Keywords:
Piplartine
Glioma
Oxidative stress
Apoptosis
Cancer therapy
Brain tumor

ABSTRACT

Piperlongumine (PL), a natural alkaloid isolated from the long pepper, may have anti-cancer properties. It selectively targets and kills cancer cells but leaves normal cells intact. Here, we reported that PL selectively killed glioblastoma multiforme (GBM) cells via accumulating reactive oxygen species (ROS) to activate JNK and p38. PL at 20 μM could induce severe cell death in three GBM cell lines (LN229, U87 and 8MG) but not astrocytes in cultures. PL elevated ROS prominently and reduced glutathione levels in LN229 and U87 cells. Antioxidant N-acetyl-L-cysteine (NAC) completely reversed PL-induced ROS accumulation and prevented cell death in LN229 and U87 cells. In LN229 and U87 cells, PL-treatment activated JNK and p38 but not Erk and Akt, in a dosage-dependent manner. These activations could be blocked by NAC pre-treatment. JNK and p38 specific inhibitors, SB203580 and SP600125 respectively, significantly blocked the cytotoxic effects of PL in LN229 and U87 cells. Our data first suggests that PL may have therapeutic potential for one of the most malignant and refractory tumors GBM.

1. Introduction

Glioblastoma multiforme (GBM), a grade IV astrocytoma, is the most common and most aggressive malignant primary brain tumor in humans. The median survival time of GBM patients is less than 14 months after routine radiation therapy and chemotherapy following resection [1]. Therefore, there is an urgent need to develop new targeted therapies and approaches to improve the clinical outcome of GBM management. GBM cells usually contain multiple gene mutations [2]. These gene mutations are important factors inducing transformation in astrocytes to become cancerous [3,4]. It is known that malignant transformation would sensitize cells to become more vulnerable to reactive oxygen species (ROS) than normal cells and therefore innovative therapy mediating ROS homeostasis is a promising strategy for treating cancers [5] including GBM.

Piperlongumine (PL) is a biological active alkaloid isolated from the long pepper (*Piper longum* L). This naturally occurring small molecule has a well-characterized structure (Fig. 1A). It has been used in Ayurvedic medicine for thousands of years for treating gastrointestinal and respiratory diseases [6]. The most recent indications of PL implied its anti-tumor effect [7,8]. In a cell-based high throughput screening study, PL was identified to be the most reliable and potent compound that can selectively kill various cancer cells and oncogene-transformed cells but not normal cells [7]. This cancer cell-sensitive cytotoxicity correlates to the selective increase of intracellular ROS in cancer cells [7]. Selective induction of ROS by PL in cancer cells represents a novel therapeutic strategy for cancers. Quantitative proteomics approach indentifies two strong PL-binding proteins, glutathione S-transerase pi 1 (GSTP1) and carbonyl reductase 1 (CBR1), which are critical in the regulation of ROS homeostasis [7]. The selective induction of ROS by PL in cancer cells represents a novel

Abbreviations: DCFH-DA, 2′-,7′-dichlorofluorescin diacetate; DMEM, Dulbecco's modified Eagle's medium; DMSO, dimethyl sulfoxide; FBS, fetal bovine serum; FCM, flow cytometry; GBM, glioblastoma multiforme; GSH, glutathione; JNK, c-jun N-terminal kinase; MTT, 3-(4,5-dimethylthiazol-2-yl)-2,5-diphenyltetrazolium bromide; NAC, N-acetyl-L-cysteine; PBS, phosphate buffered saline; PI, propidium iodide; PL, piperlongumine; ROS, reactive oxygen species.

* Corresponding author. Fax: +86 27 83692608.
E-mail address: chenxiaoqian66@gmail.com (X.Q. Chen).
[1] These authors contributed equally to the work.

0006-291X/$ - see front matter © 2013 Elsevier Inc. All rights reserved.
http://dx.doi.org/10.1016/j.bbrc.2013.06.042

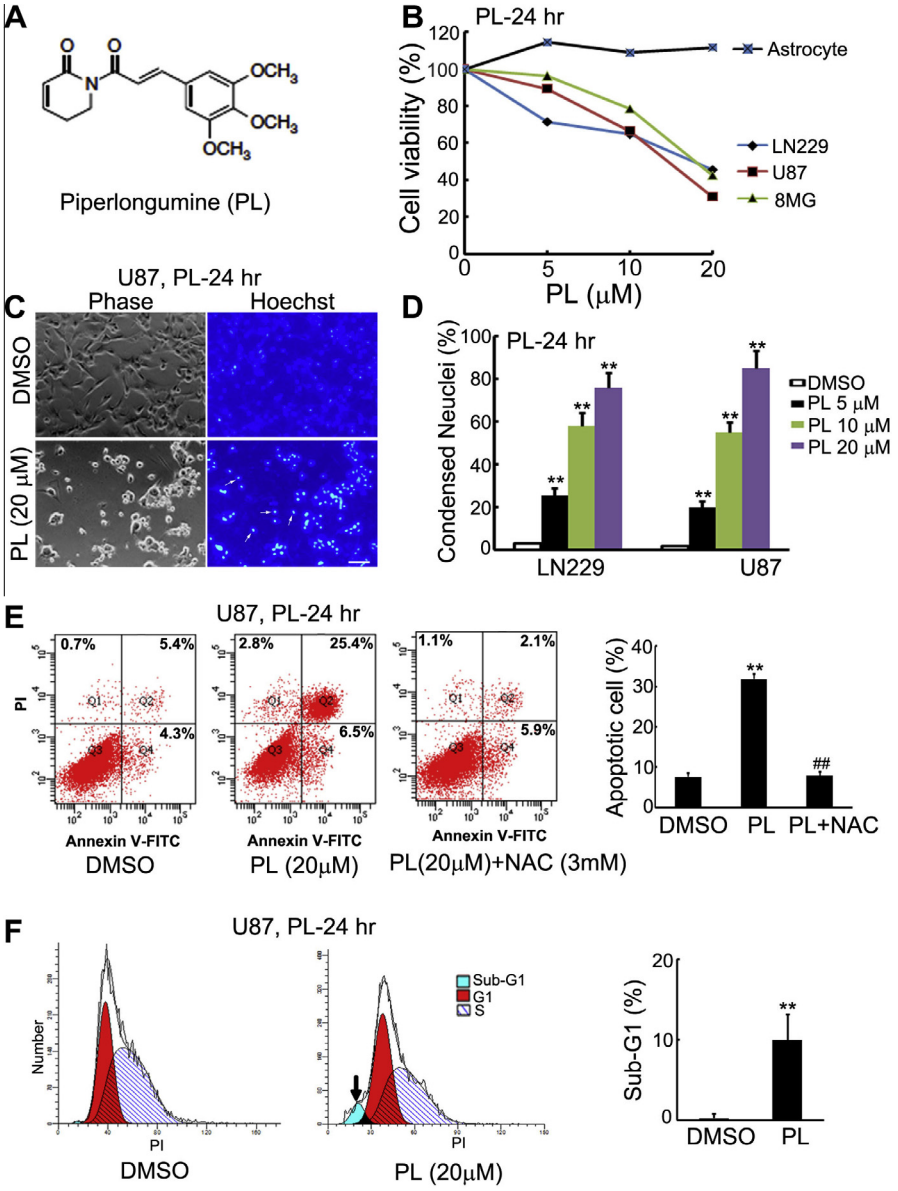

Fig. 1. PL selectively killed GBM cells but not astrocytes in cultures. (A) Chemical structure of PL. (B) PL-induced cell death in GBM cells but not astrocytes in cultures. GBM cell lines (LN229, U87 and 8MG) and cultured astrocytes were grown in 96-well plates for 24 h and treated with 0, 5, 10 and 20 μM PL for 24 h. DMSO was used as the vehicle control. Cell viability was measured by MTT assay ($n = 3$). (C) PL-induced nuclear condensation in U87 cells. U87 cells were treated with 20 μM PL for 24 h. The cultures were fixed and stained with Hoechst 33342. Representative micrographs showed the morphological changes (Phase) and nuclear condensation (indicated by arrows). Bar, 50 μm. (D) Statistical analysis of nuclear condensation in U87 cells after PL-treatment. U87 cells were treated with 5, 10 and 20 μM PL for 24 h. Photos were taken after the cultures were stained with Hoechst 33342. The percentage of condensed nuclei in total nuclei was estimated from at least 9 random fields for each culture. Data represented mean ± SEM of three independent experiments. $^{**}P < 0.01$ *vs.* corresponding DMSO control. (E) PL-induced apoptosis in U87 cells and the reversion by antioxidant NAC. U87 cells were treated with 20 μM PL alone or together with 3 mM NAC for 24 h. After Annexin V-PI double staining, cells were subjected for FCM analysis. The percentage of total apoptotic cells (Q2+Q4) was significantly increased 24 h after PL treatment but was completely reversed by NAC co-incubation. The experiments were repeated three times independently. $^{**}P < 0.01$ *vs.* DMSO and $^{\#\#}P < 0.01$ *vs.* PL. (F) PL-induced sub-G1 population in U87 cells. U87 cells were treated with 20 μM PL or DMSO for 24 h. After PI staining, cells were subjected for FCM analysis. The experiments were repeated three times independently. $^{**}P \leqslant 0.01$ vs. DMSO.

therapeutic strategy for cancers. In addition to binding GSTP1, PL exerts its anti-tumor effect by inducing protein glutathionylation upon ROS elevation [8]. PL may also induce cell cycle-arrest or induce angiogenesis in cancer cells [6].

Since PL is a natural lipophilic alkaloid amides and could pass through the blood brain barrier [9], we investigated whether PL might also be effective in killing GBM cells selectively via ROS-dependent mechanisms. Our findings suggested the potential of PL as a new therapeutic for treating this aggressive and typical fatal brain tumor.

2. Materials and methods

2.1. Cell lines

The GBM cell lines LN229, U87 MG (U87) and 8MG BA (8MG) were kindly provided by Prof. Haian Fu (Emory University, GA, USA) and were cultured in DMEM (Gibco, USA) supplemented with 5%, 10% or 20% FBS (Gibco), respectively. The cultures were used within 30 cell passages.

2.2. Primary cultures of cerebral cortical astrocytes

Protocol for the primary cultures of cerebral cortical astrocytes has been established in our laboratory [10,11]. Astrocytes grown for 4 weeks were passed to 96-well plates at a density of 1×10^6 -cells/mL. The cells in 96-well plates were used for drug treatment 7 days after subculture.

2.3. Piperlongumine and other drug treatments

Piperlongumine (PL) was purchased from Sigma (USA) and used at designated concentrations. Dimethyl sulfoxide (DMSO) of the same concentration (<1%) as in PL solutions was used as the vehicle control. N-acetyl-L-cysteine (NAC, antioxidant) (Sigma) was used at 3 mM, while SB203580 (p38 pathway specific inhibitor) and SP600125 (JNK pathway specific inhibitor) (Cell Signaling Technology, USA) were used at 10 μM. NAC, SB203580 and SP600125 were added 1 h before PL-treatment.

2.4. Cell viability or death assays

The 3-(4,5-dimethylthiazol-2-yl)-2,5-diphenyltetrazolium bromide (MTT) assay was used to measure cell viability as reported previously [12,13]. Briefly, GBM cells were seeded in 96-well plates (LN229 5000 cells/well, U87 7000 cell/well, 8MG 5000 cells/well). Twenty-four hours after seeding, cells were incubated with drugs in six parallel wells for designated times and then incubated with 20 mg/mL MTT. Cell viability was determined by optical absorption at 490 nm. Highly condensed nuclei in Hoechst 33342 staining was used to distinguish apoptotic death [11].

2.5. Flow cytometry (FCM) assay

U87 cells were treated with 20 μM PL alone or together with NAC for 24 h and co-stained with Annexin V and propidium iodide (PI) according to the manufacturer's instructions (Invitrogen, USA). Apoptotic cells were separated and quantified by a FACSCalibur Flow Cytometry System (Becton Dickinson, USA) [13]. For cell cycle assay, U87 cells were treated with 20 μM PL and stained with PI alone.

2.6. Western blotting analyses

Western blot analyses were performed as described previously [14]. Primary antibodies against p-p38 Thr180/182, p38, p-JNK Thr183/185, JNK, p-Akt Ser473, Akt, p-Erk Thr202/204, Erk were purchased from Cell Signaling Technology (USA) and β-actin antibody was from Santa Cruz Biotechnology (USA). The blots were visualized with corresponding fluorescent secondary antibodies and the bands were quantified by using the Odyssey Infrared Imaging System (Li-COR Bioscience, USA).

2.7. Quantification of reduced glutathione (GSH)

Cells were treated with PL alone or together with NAC for 1 h, then washed with ice-cold PBS three times and collected in centrifuge tubes. After sonification for 2–3 min on ice, cell lysates were centrifuged at 3500 rpm at 4 °C for 10 min and the supernatants were collected for GSH measurement according to the manufacture's protocol (A006–2, Nanjing Jiangcheng Bioengineering Institute, China) using a microplate reader at 405 nm (Synergy 2, BioTek, USA). The concentration of GSH was calculated according to the manufacturer's instructions (A006-2, Nanjing Jiangcheng Bioengineering Institute). Relative GSH levels in PL-treated cells were expressed as fold change relative to DMSO control.

2.8. Measurement of ROS production

Cells were treated with PL for 1 or 3 h alone or together with other drugs and the ROS level was detected using 2′-,7′-dichlorofluorescin diacetate (DCFH-DA) (Sigma). In brief, cells were incubated with 10 μM of DCFH-DA for 30 min at 37 °C, and washed twice with PBS before photographing under a conventional fluorescent microscope (Olympus, Japan). For each culture, a minimum of 9 random fields were captured. Average fluorescent intensity was analyzed using the Image-Pro Plus software (Media Cybernetics, USA).

2.9. Statistical analyses

All experiments were repeated independently at least three times. The values were expressed as mean ± SEM and statistics were performed with a 2-way ANOVA followed by the Student–Newman–Keuls test. *P* values of less than 0.05 were considered statistically significant.

3. Results

3.1. Piperlongumine selectively kills GBM cell lines but not astrocytes in cultures

We tested the cytotoxic effects of PL in three different GBM cell lines (LN229, U87 and 8MG) with different genetic backgrounds to evaluate the therapeutic potential of PL for GBM. MTT assays demonstrated that 24 h PL-treatment could significantly increase cell death in all three GBM cell lines and the effects were dose-dependent (Fig. 1B). IC50 of PL in LN229, U87 MG and 8MG cells was in the range of 10–20 μM. However, PL even at 20 μM did not affect the viability of astrocytes in cultures (Fig. 1B). PL at 40 μM would kill both GBM cells and astrocytes to a similar extent (data not shown). We also examined PL-induced cell death in LN229 and U87 cells by examining cell morphology and nuclear staining. Fig. 1C showed the morphological and nuclear changes of U87 cells after 24 h of 20 μM PL-treatment. PL-treatment induced severe nuclear condensation and cell death (Fig. 1C). The percentage of cells with highly condensed nuclei (representing programmed cell death) [11,14] significantly increased in both LN229 and U87 cells subjected to 5, 10 and 20 μM PL-treatments (Fig. 1D).

PL-induced apoptotic cell death in U87 cells was further verified with Annexin V and PI double staining (Fig. 1E). FCM results showed that there was a prominent increase of late apoptotic cells (25.4%, with higher Annexin V and PI signals in quadrant 2, Q2) in U87 cells after treated with 20 μM PL for 24 h as compared to that of DMSO control (5.4%) (Fig. 1E). Cells in quadrant 4 (Q4) with higher Annexin V but lower PI signals represented cells at an earlier apoptotic stage. The percentage of total apoptotic cells (Q2+Q4) was significantly increased in U87 cells after 24 h of 20 μM PL-treatment (Fig. 1E). Antioxidant NAC co-incubation could completely block the PL-induced apoptosis in U87 cells (Fig. 1E). Further, cell cycle assay demonstrated that PL significantly increased U87 cells in the sub-G1 stage after 24 h of 20 μM PL-treatment (Fig. 1F).

3.2. Piperlongumine induces ROS accumulation in GBM cells

Previous studies have indicated that PL plays a major role in disturbing ROS homeostasis [7]. DCFH-DA is the most common ROS detection reagent which generates fluorescence in the presence of ROS. The DCFH-DA fluorescent intensities in cells correlate well to cellular ROS levels. DCFH-DA fluorescent intensities were enhanced prominently in LN229 and U87 cells after treatment with

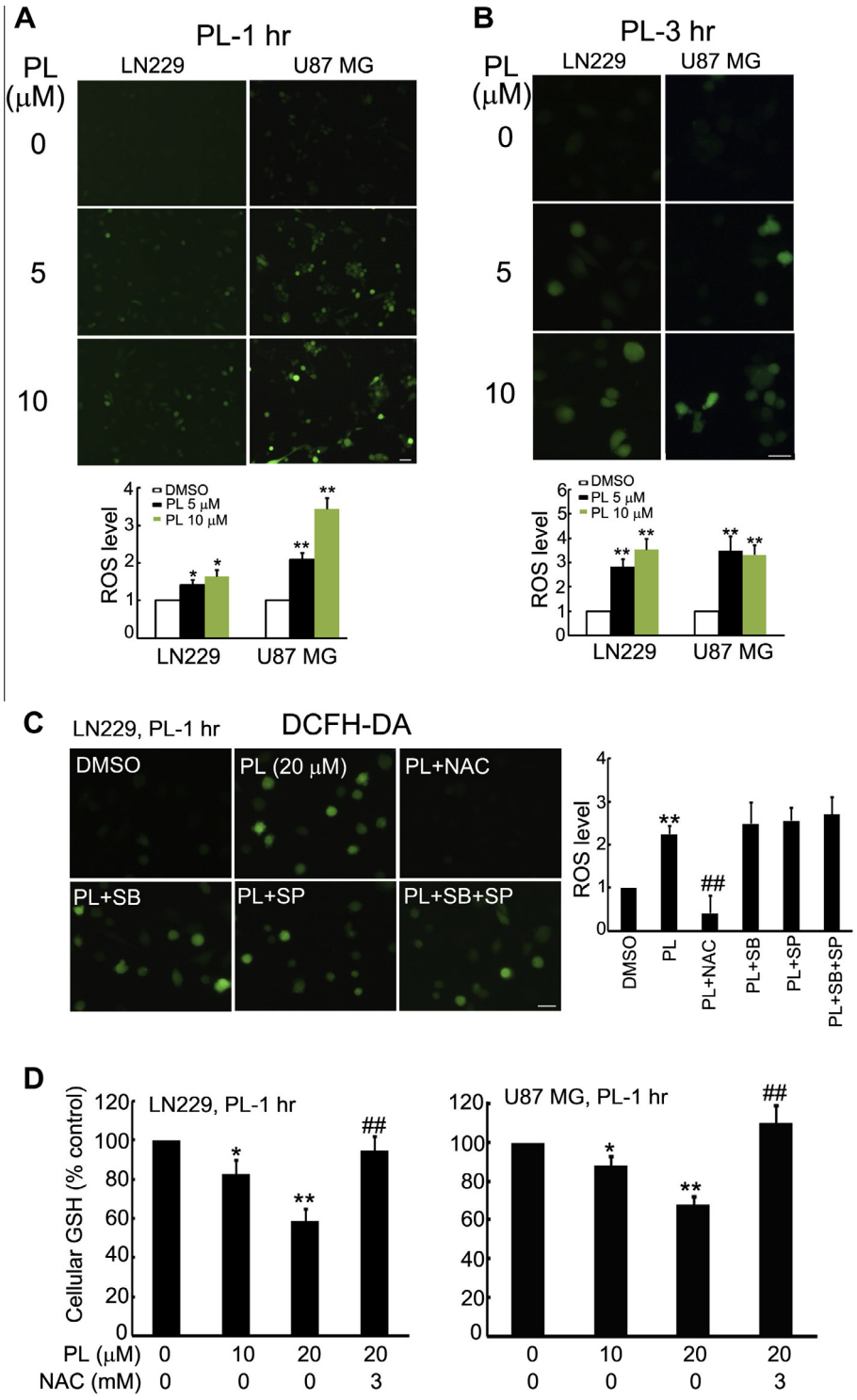

Fig. 2. PL induces ROS accumulation in GBM cells. (A) ROS elevation in GBM cells 1 h after PL-treatment. LN229 or U87 cells were treated with PL for 1 h and stained with DCFH-DA. Representative micrographs showed that the fluorescent intensity of DCFH-DA was enhanced after PL treatment. Bar, 20 μm. For statistical analysis, the mean DCFH-DA fluorescent intensity (representing cellular ROS level) was measured from 9 random fields for each culture. All values represented mean ± SEM of three independent experiments. $^{*}P < 0.05$ and $^{**}P < 0.01$ *vs.* corresponding DMSO control. (B) ROS elevation in LN229 and U87 cells 3 h after PL-treatment. $^{*}P < 0.05$ and $^{**}P < 0.01$ *vs.* corresponding DMSO control. (C) NAC but not JNK/p38 inhibitors reversed PL-induced ROS elevation in LN229 cells. LN229 cells were treated with 20 μM PL alone or co-treated with 3 mM NAC, 10 μM SP600125, 10 μM SB203580, or 10 μM SP600125+10 μM SB203580 for 1 h. Fluorescent micrographs were taken 30 min after DCFH-DA staining. Bar, 20 μm. $^{**}P < 0.01$ *vs.* DMSO control and $^{\#\#}P < 0.01$ *vs.* PL alone. (D) PL-reduced GSH in GBM cells. LN229 or U87 cells were treated with 10 or 20 μM PL for 1 h and then the cellular GSH level was measured. NAC was pretreated for 1 h and then co-treated with PL for another 1 h. Data represented mean ± SEM of three independent experiments. $^{*}P < 0.05$, $^{**}P < 0.01$ *vs.* corresponding DMSO control. $^{\#\#}P < 0.01$ *vs.* PL (20 μM).

5 and 10 μM PL for 1 h (PL-1 h, Fig. 2A) and 3 h (PL-3 h, Fig. 2B). The fluorescent intensities were semi-quantified and the statistical analyses demonstrated the relative cellular ROS levels (i.e., DCFH-DA fluorescent intensity) were significantly increased at 1 h (lower panel, Fig. 2A) and 3 h (lower panel, Fig. 2B) after 5 and 10 μM PL-treatments in both LN229 and U87 cells. Co-incubation with 3 mM NAC and 20 μM PL (PL+NAC) completely reversed the effect of PL on ROS increase in LN229 cells (left panels, Fig. 2C). Statistical analyses confirmed that cellular ROS level increased significantly at 1 h of 20 μM PL-treatments as compared to that of DMSO control, whereas and the PL-induced ROS was abolished when co-treated with NAC (right panel, Fig. 2C). Consistent to the increase of ROS, treatment with PL for 1 h significantly reduced cellular GSH levels in LN229 (left panel, Fig. 2D) and U87 cells (right panel, Fig. 2D). The reduction of GSH could be prevented in the presence of NAC (Fig. 2D). These data demonstrated that PL induced ROS accumulation in GBM cells.

3.3. Piperlongumine activates p38 and JNK in GBM cells in a dosage-dependent manner

We examined the effects of PL on JNK and p38 activation, two canonical ROS-activated signaling proteins that control cell death under oxidative stress [15,16]. Western blotting results showed a dosage-dependent increase in both p-JNK and p-p38 levels in LN229 cells 6 h after PL-treatment (Fig. 3A). The expression level of p-JNK but not p-p38 in LN229 cells at 12 h of PL-treatment was evidently reduced from that at 6 h (Fig. 3A). Interestingly, PL had no effect on Akt and Erk phosphorylation (Fig. 3B), two key aberrant oncogenic signaling proteins in GBM cells [2] reported to be involved in PL's biological activities [6]. In U87 cells, the peak expression levels of p-p38 and p-JNK appeared 3 h after PL-treatment (Fig. 3C). PL also induced a dosage-dependent p38 activation in U87 cells 3 h after PL-treatment (Fig. 3D). Notably, JNK activation was more prominent in LN229 cells (Fig. 3A) while p38 activation was more prominent in U87 cells (Fig. 3C and D), likely attributed to the different genetic backgrounds of LN229 and U87 cells. Co-incubation of PL and NAC completely blocked PL-induced activation of JNK in LN229 (Fig. 3E) and activation of both p38 and JNK in U87 cells (Fig. 3F), suggesting that PL-induced p38 and JNK activation was ROS-dependent.

3.4. Piperlongumine induces GBM cell death via ROS-dependent p38 and JNK activation

We further clarified the relationship of ROS elevation, p38 and JNK activation to PL-induced cell death in GBM cell lines. SP600125 and SB203580 are specific JNK and p38 pathway inhibitors, respectively. Western blotting analyses demonstrated that PL-induced JNK activation in LN229 (Fig. 4A) was completely suppressed by 10 μM of SP600125. SB203580 is known to suppress downstream targets of p-p38 [17,18] and it only partially

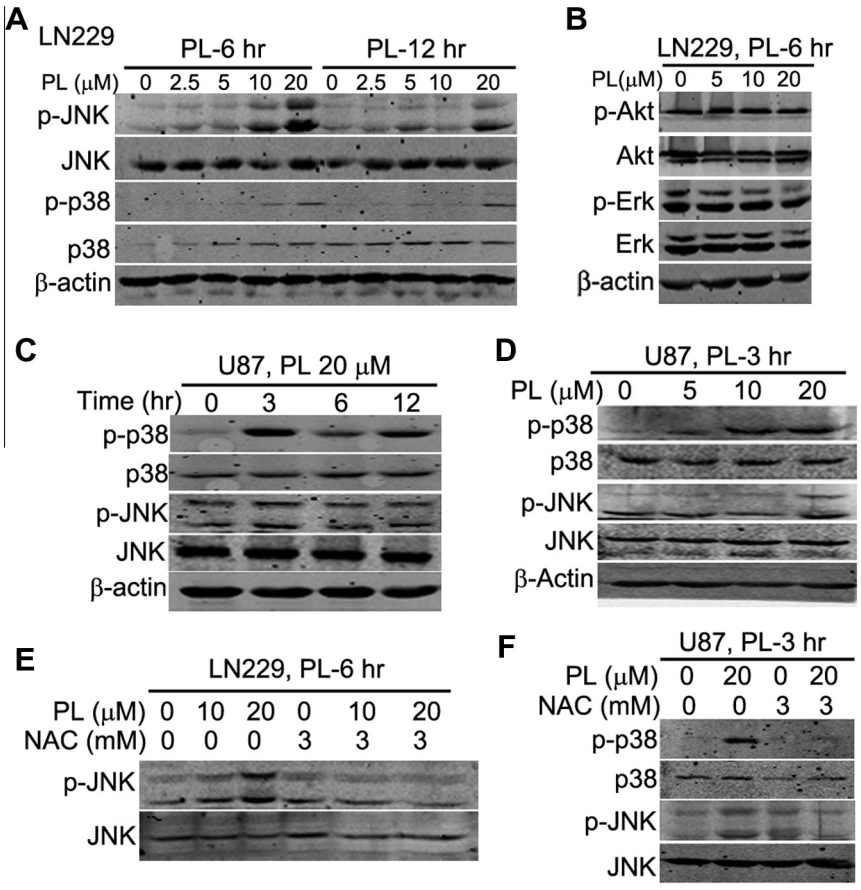

Fig. 3. PL induces JNK and p38 activation in GBM cells. (A) Representative Western blots of JNK and p38 phosphorylation in PL-treated LN229 cells. LN229 cells were treated with 0, 2.5, 5, 10, 20 μM PL for 6 and 12 h. Equal amounts of total proteins were subjected for Western blotting analysis with designated antibodies. (B) Representative Western blots of p-Akt/Akt and p-Erk/Erk in PL-treated LN229 cells. (C) Representative Western blots of p-JNK/JNK and p-p38/p38 in PL-treated U87 cells at various time points. (D) Representative Western blots of p-p38/p38 and p-JNK/JNK 3 h after various dosages of PL-treatment in U87 cells. (E) Representative Western blots of the NAC effects on PL-induced JNK phosphorylation in LN229 cells. (F) Representative Western blots of the effects of NAC on PL-induced p38 and JNK phosphorylation in U87 cells. All experiments were repeated in three independent experiments.

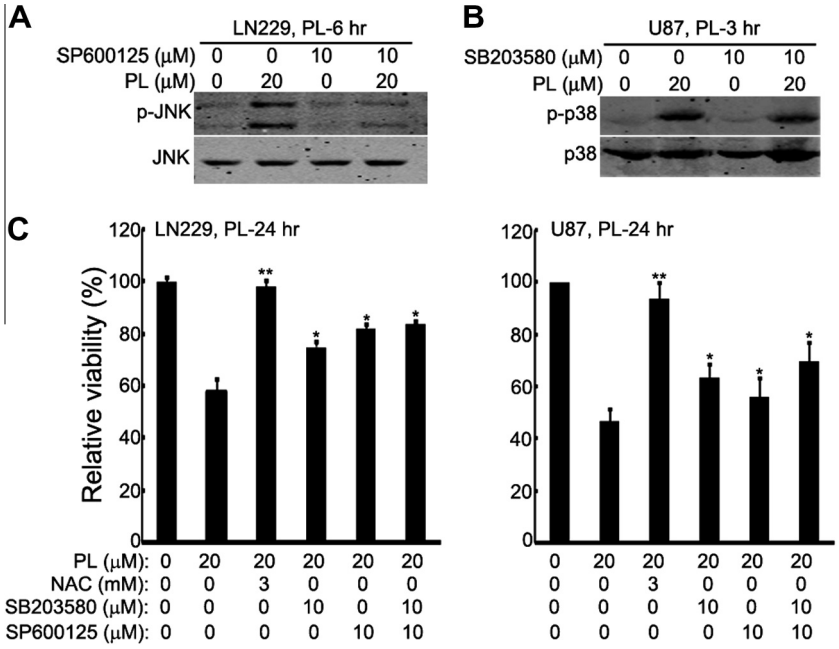

Fig. 4. Activation of JNK and p38 contributes to PL-induced GBM cell death. (A) Representative Western blots of the effects of SP600125 on PL-induced JNK activation in LN229 cells. (B) Representative Western blots of the effects of SB203580 on PL-induced p38 activation in U87 cells. (C) Statistical analysis of the effects of SB203580, SP600125 or NAC on the cell viability of GBM cells. LN229 or U87 cells were treated with PL alone or co-treated with 3 mM NAC, 10 μM SB203580, 10 μM SP600125, or 10 μM SB203580 + 10 μM SP600125 for 24 h. Cell viability was determined by MTT assay. Data represented mean ± SEM of three independent experiments. $^{*}P < 0.05$ and $^{**}P < 0.01$ *vs.* corresponding control (PL 0 μM).

suppressed p-p38 level in U87 MG cells (Fig. 4B). MTT assays demonstrated that the cell viability improved when SB203580 or SP600125 was co-incubated with PL in LN229 (left panel, Fig. 4C) and U87 cells (right panel, Fig. 4C). Treatment alone or in combination with 10 μM SB203580 and 10 μM SP600125 only partially prevented PL-induced cell death (Fig. 4C). However, co-incubation with NAC completely prevented PL-induced apoptosis in U87 cells as measured by FCM assay (Fig. 1E) and PL-induced cell death in both LN229 and U87 MG cells as measured by MTT assay (Fig. 4C). Inhibition of JNK pathways by 10 μM SB203580 or p38 pathways by 10 μM SP600125 did not significantly alter DCFH-DA fluorescent intensities in PL-treated LN229 cells (Fig. 2C). Therefore, p38 and JNK appeared to function as downstream targets of ROS elevation upon PL-treatment.

4. Discussion

In the present study, we demonstrated that PL was effective in killing GBM cells via ROS-mediated p38 and JNK pathways.

PL is a natural alkaloid amide with many medical applications [6]. Recently, PL was found to be a promising anticancer compound [7]. Some previous studies have shown that PL may not be effective in killing all kinds of cancer cells [6]. Due to its lipophilic property and novel anti-cancer indications, it would be interesting to investigate whether PL is also effective in killing GBM, an incurable brain tumor. Our results indicated that PL selectively killed GBM cell lines but not normal astrocytes implying PL's potential of becoming an effective drug for treating GBM (Fig. 1). ROS appears to be the key player in PL-induced cell death in cancer [7]. However, some discrepancies in the PL cytotoxic effect and its ROS-induction property have been also reported in some cancer cells [8]. Results from our NAC experiments confirmed that PL kills GBM cells via inducing ROS formation and accumulation. It is reported that PL binds preferentially to enzymes (such as GSTP1 and CBR1) participating in the cellular responses to oxidative stress in EJ and U2OS cells [7]. Overexpression of either GSTP1 or CBR1 reduces PL-induced ROS and cell death [7]. However, knockdown of GSTP1 or CBR1 has no effect on PL-induced ROS and cell death, suggesting that there are other proteins involved in PL-induced ROS accumulation [7]. Whether PL elevates ROS via binding to GSTP1 and CBR1 in GBM cells requires further investigation.

The signaling pathways participated in PL-induced cancer cell death remain elusive. We noticed an early and prominent activation of both JNK and p38, two typical ROS-responsive pathways, in GBM cells under PL-treatment. Antioxidant NAC blocked ROS induction, JNK and p38 activation, while inhibitors of JNK or p38 significantly blocked PL-induced cell death (Fig. 4) but not ROS induction (Fig. 3). Therefore, JNK and p38 are two downstream effectors of PL-induced ROS in GBM cells. It is known that GSTP1 is a negative regulator of JNK [19]. Thus, PL might activate JNK by quenching GSTP1 activities in GBM cells. In addition to p38 and JNK pathways, we also investigated other proposed pathways potentially involved in PL's bioactivities, such as Erk [20] and Akt [21]. To our surprise, we did not observe any changes of p-Erk and p-Akt in LN229 cells under PL-treatment (Fig. 3B). This suggests that PL selectively activates JNK and p38 pathways in GBM cells. We did not study other possible mechanisms such as protein glutathionylation [8] and proteosome degradation [22] which might be involved in PL-induced GBM cell death. Understanding and clarifying the molecular mechanisms of PL in the future is essential to validate the suitability of PL for treating GBM.

In summary, we have demonstrated that PL induces selective cell death in GBM cell lines via ROS accumulation. Importantly, we have discovered that p38 and JNK activation are involved in PL-induced GBM cell death. Our data provide the first experimental evidence in supporting PL as a potential therapeutic for treating GBM.

Acknowledgments

We thank Dr. Ann Y.K. Wong for her helpful comments on the manuscript. This work was supported by the National Natural

Science Foundation of China (Grants 30570555, 81070937, 81172397, 81201726 and 31271444).

References

[1] R. Stupp, W.P. Mason, M.J. van den Bent, M. Weller, B. Fisher, M.J. Taphoorn, K. Belanger, A.A. Brandes, C. Marosi, U. Bogdahn, J. Curschmann, R.C. Janzer, S.K. Ludwin, T. Gorlia, A. Allgeier, D. Lacombe, J.G. Cairncross, E. Eisenhauer, R.O. Mirimanoff, Radiotherapy plus concomitant and adjuvant temozolomide for glioblastoma, N. Engl. J. Med. 352 (2005) 987–996.

[2] Comprehensive genomic characterization defines human glioblastoma genes and core pathways, Nature 455 (2008) 1061–1068.

[3] S.M. Evans, K.D. Judy, I. Dunphy, W.T. Jenkins, W.T. Hwang, P.T. Nelson, R.A. Lustig, K. Jenkins, D.P. Magarelli, S.M. Hahn, R.A. Collins, M.S. Grady, C.J. Koch, Hypoxia is important in the biology and aggression of human glial brain tumors, Clin. Cancer Res. 10 (2004) 8177–8184.

[4] S. Zhao, Y. Lin, W. Xu, W. Jiang, Z. Zha, P. Wang, W. Yu, Z. Li, L. Gong, Y. Peng, J. Ding, Q. Lei, K.L. Guan, Y. Xiong, Glioma-derived mutations in IDH1 dominantly inhibit IDH1 catalytic activity and induce HIF-1alpha, Science 324 (2009) 261–265.

[5] D. Trachootham, J. Alexandre, P. Huang, Targeting cancer cells by ROS-mediated mechanisms: a radical therapeutic approach?, Nat Rev. Drug Discov. 8 (2009) 579–591.

[6] D.P. Bezerra, C. Pessoa, M.O. de Moraes, N. Saker-Neto, E.R. Silveira, L.V. Costa-Lotufo, Overview of the therapeutic potential of piplartine Piperlongumine, Eur. J. Pharm. Sci. 48 (2012) 453–463.

[7] L. Raj, T. Ide, A.U. Gurkar, M. Foley, M. Schenone, X. Li, N.J. Tolliday, T.R. Golub, S.A. Carr, A.F. Shamji, A.M. Stern, A. Mandinova, S.L. Schreiber, S.W. Lee, Selective killing of cancer cells by a small molecule targeting the stress response to ROS, Nature 475 (2011) 231–234.

[8] D.J. Adams, M. Dai, G. Pellegrino, B.K. Wagner, A.M. Stern, A.F. Shamji, S.L. Schreiber, Synthesis, cellular evaluation, and mechanism of action of piperlongumine analogs, Proc. Natl. Acad. Sci. USA 109 (2012) 15115–15120.

[9] H. Liu, R. Luo, X. Chen, J. Liu, Y. Bi, L. Zheng, X. Wu, Tissue distribution profiles of three antiparkinsonian alkaloids from Piper longum L. in rats determined by liquid chromatography-tandem mass spectrometry, J. Chromatogr. B Analyt. Technol. Biomed. Life Sci. 928 (2013) 78–82.

[10] X.Q. Chen, J.G. Chen, Y. Zhang, W.W. Hsiao, A.C. Yu, 14–3-3gamma is upregulated by in vitro ischemia and binds to protein kinase Raf in primary cultures of astrocytes, Glia 42 (2003) 315–324.

[11] X.Q. Chen, L.Y. Qin, C.G. Zhang, L.T. Yang, Z. Gao, S. Liu, L.T. Lau, Y.W. Fung, D.A. Greenberg, A.C. Yu, Presence of neuroglobin in cultured astrocytes, Glia 50 (2005) 182–186.

[12] S.Q. Ye, X.Y. Zhou, X.J. Lai, L. Zheng, X.Q. Chen, Silencing neuroglobin enhances neuronal vulnerability to oxidative injury by down-regulating 14–3-3gamma, Acta Pharmacol. Sin. 30 (2009) 913–918.

[13] J. Zhang, S.J. Lan, Q.R. Liu, J.M. Liu, X.Q. Chen, Neuroglobin, a novel intracellular hexa-coordinated globin, functions as a tumor suppressor in hepatocellular carcinoma via Raf/MAPK/Erk, Mol. Pharmacol. 83 (2013) 1109–1119.

[14] X.Q. Chen, A.C. Yu, The association of 14–3-3gamma and actin plays a role in cell division and apoptosis in astrocytes, Biochem. Biophys. Res. Commun. 296 (2002) 657–663.

[15] M. Gomez-Lazaro, M.F. Galindo, R.M. Melero-Fernandez de Mera, F.J. Fernandez-Gomez, C.G. Concannon, M.F. Segura, J.X. Comella, J.H. Prehn, J. Jordan, Reactive oxygen species and p38 mitogen-activated protein kinase activate Bax to induce mitochondrial cytochrome c release and apoptosis in response to malonate, Mol. Pharmacol. 71 (2007) 736–743.

[16] D. Xiao, Y. Zeng, L. Prakash, V. Badmaev, M. Majeed, S.V. Singh, Reactive oxygen species-dependent apoptosis by gugulipid extract of Ayurvedic medicine plant *Commiphora mukul* in human prostate cancer cells is regulated by c-Jun N-terminal kinase, Mol. Pharmacol. 79 (2011) 499–507.

[17] S. Kumar, M.S. Jiang, J.L. Adams, J.C. Lee, Pyridinylimidazole compound SB 203580 inhibits the activity but not the activation of p38 mitogen-activated protein kinase, Biochem. Biophys. Res. Commun. 263 (1999) 825–831.

[18] C.I. Schwer, M. Mutschler, P. Stoll, U. Goebel, M. Humar, A. Hoetzel, R. Schmidt, Carbon monoxide releasing molecule-2 inhibits pancreatic stellate cell proliferation by activating p38 mitogen-activated protein kinase/heme oxygenase-1 signaling, Mol. Pharmacol. 77 (2010) 660–669.

[19] T. Wang, P. Arifoglu, Z. Ronai, K.D. Tew, Glutathione S-transferase P1–1 (GSTP1-1) inhibits c-Jun N-terminal kinase (JNK1) signaling through interaction with the C terminus, J. Biol. Chem. 276 (2001) 20999–21003.

[20] H. Randhawa, K. Kibble, H. Zeng, M.P. Moyer, K.M. Reindl, Activation of ERK signaling and induction of colon cancer cell death by piperlongumine, Toxicol. In Vitro 27 (2013) 1626–1633.

[21] D.J. Son, S.Y. Kim, S.S. Han, C.W. Kim, S. Kumar, B.S. Park, S.E. Lee, Y.P. Yun, H. Jo, Y.H. Park, Piperlongumine inhibits atherosclerotic plaque formation and vascular smooth muscle cell proliferation by suppressing PDGF receptor signaling, Biochem. Biophys. Res. Commun. 427 (2012) 349–354.

[22] M. Jarvius, M. Fryknas, P. D'Arcy, C. Sun, L. Rickardson, J. Gullbo, C. Haglund, P. Nygren, S. Linder, R. Larsson, Piperlongumine induces inhibition of the ubiquitin-proteasome system in cancer cells, Biochem. Biophys. Res. Commun. 431 (2013) 117–123.